OPERATING BEHAVIOR OF A PHOTOVOLTAIC-DRIVEN ELECTROLYSIS SYSTEM

Gero Walter – Gero.Walter@Carissma.eu
Sergej Diel
Carlos Antônio Rufino Júnior
Hans-Georg Schweiger
Technische Hochschule Ingolstadt, CARISSMA Institute of Electric, Connected and Secure Mobility
Iury Valente de Bessa
Federal University of Amazonas, Department of Electricity
Maíra Mallmann
Aline Kirsten Vidal de Oliveira
Daniel Odilio Dos Santos
Ricardo Rüther
Universidade Federal da Santa Catarina, Fotovoltaica Solar Energy Research Laboratory

Abstract. *Increasing demand for clean and sustainable energy is always accompanied by the challenge of storage and transportation. Hydrogen is a promising solution for storing energy generated by solar photovoltaics (PV). The intermittent nature of PV power generation systems represents a particular challenge for coupled water electrolysis systems. Batteries can be connected in parallel with the power generation system to mitigate the intermittency of renewable sources and to reduce the nominal power of electrolyzers and, consequently, the costs. The analysis of operational behavior is the first stage of designing an algorithm for PV power generation systems composed of water electrolyzers connected with batteries in parallel with a PV power generation system. This algorithm can identify the optimal operational points for the operation. This paper analyzes the energy demand under real operating conditions of an Anion Exchange Membrane (AEM) electrolyzer and the energy required for startup. To achieve this objective, the behavior under various production rates and electrolyte temperatures following different durations of idle phases were examined. An analysis of the dynamic response was also carried out. Significant amounts of energy are required for startup, particularly during high production rates and cold starts. From an operating time of around 3 hours after starting, the startup energy no longer plays a major role. The fast dynamic response of AEM electrolyzers also makes it possible to follow the intermittent supply from PV systems. Based on this, the energy budget for hydrogen production can be determined over the operating time, considering the startup. These results can support the development of control algorithms for the optimal operation of these green hydrogen production systems.*

Keywords: *Hydrogen Water Electrolysis, Solar Energy, AEM Electrolysis*

1. INTRODUCTION

Brazil is a country that receives a high level of solar radiation, which makes it suitable for generating clean and sustainable energy through renewable energy generation systems such as solar and wind energy. Photovoltaic systems generate electricity by converting solar energy. This process frequently results in energy generation at intermittent supply. As a result, battery systems can be efficiently used to store excess energy produced during periods of low demand, and to supply any shortfall caused by the intermittent availability of solar radiation. Subsequently, this accumulated energy can be transferred to the electrical grid during periods of high demand, a technique commonly known as peak shaving. While the coupling of PV with pure battery storage is advantageous for short-term storage, the combination of water electrolysis, hydrogen storage and fuel cells for the later regeneration of electricity is advantageous for storage over longer periods of time due to the very low self-discharge losses of hydrogen storage systems (Arsalis *et al*., 2022). This application is very interesting in the context of countries that have low hydrogen production costs, such as Brazil (McKinsey, 2021), including the isolated systems in the Amazon region, supplied by costly and polluting alternatives such as diesel generation.

Off-grid applications are a solution for isolated communities, such as those in the Amazon. As Instituto de Energia e Meio Ambiente (2022) showed, more than 990,000 Brazilians in the Amazon region were living without a connection to the electricity grid in 2019. Current electrification projects in this region mainly use diesel generators, PV systems in combination with batteries and hybrid systems with both technologies (Leduchowicz-Municio *et al.,* 2022). In off-grid systems without connection to the electricity grid, hydrogen can be used as an energy carrier. In these systems, the energy generated by photovoltaics produces hydrogen through water electrolysis. Water electrolysis involves splitting water molecules into hydrogen and oxygen using an electrical current. The hydrogen produced through this process can be stored and converted into electricity using a fuel cell. The fuel cell is a device that combines hydrogen and oxygen to

produce electricity, with water as the only by-product. This electricity can supply the community with power, even in remote areas with limited grid access. Such PV-fed off-grid systems are beneficial for storing energy during seasonal fluctuations, such as the rainy season. This allows for a more reliable and continuous electricity supply in off-grid communities. These systems are particularly suitable if storage is to be based on seasonal fluctuations such as the rainy season (Mayyas *et al.*, 2020). However, the application of these systems has been limited due to cost factors, as highlighted in a case study on supplying isolated communities in Brazil (Silva *et al.*, 2013). The cost of PV modules and electrolyzers used in the water electrolysis process has been a barrier to the widespread adoption of such systems. In a recent analysis, Oliveira *et al.* (2023) investigated the potential of such a system for the municipality Izidolândia in the Amazon. The analysis showed that existing hydrogen systems are not yet economically competitive with battery storage for off-grid energy storage in the Amazon region. The costs of the hydrogen components would have to be reduced by around 90 % to become economically competitive. With increasing market scale and technology improvements, both solar PV and Li-ion batteries have experienced comparable cost reductions over the past decade.

Water electrolysis systems can also be used to produce pure hydrogen. In this case, the hydrogen produced is not converted back into electricity using a fuel cell on-site but is used in other sectors. These can include transportation, industry, or heat generation (Zeyen *et al.*, 2023). Applying PV-fed water electrolysis systems in these sectors offers advantages, as it allows for independent hydrogen production without relying on the grid. When green hydrogen is produced from renewable energy sources, hydrogen generation is subject to the intermittency of these sources. To ensure continuous operation of the electrolyzers, energy would need to be drawn from the grid during times of low energy supply from renewable sources. However, by utilizing PV-fed water electrolysis systems, the need to draw energy from the grid can be minimized or eliminated, as the system can directly utilize the energy generated by the PV panels for electrolysis. This allows for constant operation of the electrolyzers, even during periods of low energy supply from the grid or renewable sources. The ability to produce hydrogen independently of the grid is advantageous, as it reduces reliance on external energy sources and increases the sustainability of hydrogen production. Furthermore, it does not place any additional load on the electricity grid.

Both off-grid technologies share a complex set of costs. The costs of the individual system components consisting of PV modules, batteries, electrolyzer and, if applicable, fuel cells have a major influence on the overall costs of the system (Kikuchi *et al.*, 2019). If the electrolyzer is not operated with battery buffering, it must be designed for the expected peak load of the PV system. This is usually only reached over a short period during the day. The rest of the time, the electrolyzer is only operated in a low load range. However, the costs for electrolyzers with a high nominal power are higher than for electrolyzers with lower nominal power. In unbuffered PV-fed operation, the electrolyzer has to be shut-down at night due to a lack of renewable energy. This reduces the utilization factor which is important for the cost efficiency analysis. The utilization factor is the ratio of the electrolyzer being in full use to the day's total time. If the electrolyzer is only active at full power for a short period of time during the daylight hours, the utilization ratio is low. Therefore, battery buffering can improve the utilization factor. During the day, only a defined proportion of the PV system's power is delivered to the electrolyzer. The remaining energy is supplied to the battery. At night, when there is no sunshine, the electrolyzer is powered by energy from the battery. Papadoulos *et al.* (2018) and Kikuchi *et al.* (2019) show that using batteries as buffer storage increases the utilization of the electrolyzer and thus reduces the costs of hydrogen production. Becker *et al.*, (2021) are investigating the possibility of increasing the battery capacity to such a level that the stored energy is sufficient to operate the alkaline electrolysis during the whole night, which works with renewable energy generation in Morocco in that study.

Depending on the type of electrolyzer selected, intermittent operation can also significantly impact efficiency and degradation. Currently, mostly four types of electrolyzers are commercially available. These are Alkaline Electrolysis (AEL) with a liquid basic electrolyte, acid electrolysis with a Polymer Solid Electrolyte (Proton Exchange Membrane Electrolysis, PEMEL), electrolysis using an Alkaline Anion exchange membrane (Anion Exchange Membrane Electrolysis, AEMEL) and high-temperature electrolysis with a Solid Oxide Ceramic as Electrolyte (Solid Oxide Ceramic Electrolysis, SOEC or SOEL) (Shiva Kumar and Lim, 2022). Alkaline electrolysis is already being used commercially on a large scale (Kuckshinrichs *et al.*, 2017). As no noble metals are required for the electrolyzer, it has moderate investment costs. A limiting factor is the low current density (Shiva Kumar and Himabindu, 2019). Using PEM electrolyzers allows for high-current densities, efficiency and purity of the hydrogen produced (Shiva Kumar and Himabindu, 2019). At the same time, the noble metals used to manufacture PEM electrolyzers makes the technology very expensive (Neugebauer, 2022). The use of solid oxide electrolyzers enables even higher efficiencies and hydrogen purity. For this purpose, electrolysis is carried out at operating temperatures around 500 - 850 °C. It is also possible to thermally integrate solid oxide water electrolysis with downstream chemical synthesis, i.e., methanol synthesis (Khan *et al.*, 2018; Shiva Kumar and Lim, 2022). Anion Exchange Membrane Electrolyzers (AEMEL) are a technology that has been researched more intensively in recent years. These mostly combine the concepts of AEL and PEMEL. The electrochemical mode of operation of AEM is comparable to that of AEL. As shown in Fig. 1, distilled water or very small doses of potassium hydroxide solution are added to the cathode for AEMEL. As in alkaline electrolysis, hydrogen and hydroxide ions (OH^-) are formed at the cathode by electron uptake, which migrate to the anode and react to form oxygen by electron release (Khan *et al.*, 2018; Neugebauer, 2022). This work revolves in the operating behavior of operating AEM electrolyzers in a laboratory environment. So far, there is little experience with the continuous use of

commercial AEMEL. Based on initial field experience, AEMEL manufacturer *Enapter* states that frequent start/stop cycles can accelerate degradation of its electrolyzers. The ideal efficiency and longest service life can be achieved in continuous operation (Enapter (1), 2023).
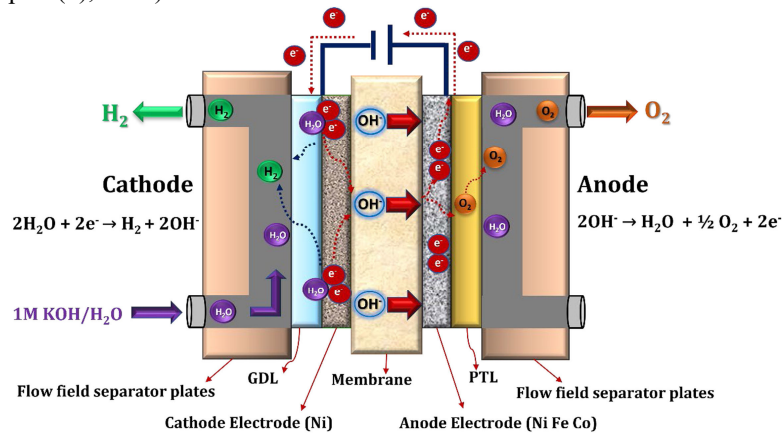

Figure 1- Schematic view of AEM water electrolysis working principle *(Shiva Kumar and Lim, 2022)*.

For the battery storage, various types of batteries can be applied. Previously considered types are i.e. lead-acid battery banks (Tebibel *et al*., 2017) or Li-Ion Batteries (LIBs) (Arsalis *et al*., 2022). Especially when using LIBs, the use of second-life batteries can be an interesting alternative. These are usually batteries previously used as traction batteries in Battery Electric Vehicles (BEVs). As they age, decreasing energy density makes their use no longer sensible in mobile applications. However, they can still safely be used in stationary applications. Falk *et al*. (2020) showed that a second-life LIB can be useful for PV island systems. With a rapidly growing market for electric vehicles, the market for second-life batteries is also expected to grow strongly within the next few years (Zhao *et al*., 2021). A meaningful application of second use is also conceivable for the battery buffering of water electrolysis systems.

In addition to the possibility of designing the electrolyzers for a lower nominal output, battery-buffering can also help avoiding the energy consumption of the startup process by continuous operation. This process includes the energy consumption of all peripheral systems required for operation and the electrolyzer before hydrogen is produced. The energy requirement depends mainly on the selected electrolyzer technology. High-temperature electrolyzers work at very high operating temperatures requiring more time and energy during startup. Other electrolyzers work at lower temperatures and therefore require less energy and take less time to start up. However, all types have in common that a certain amount of energy must be supplied before hydrogen can be produced. These processes must be considered when developing a control system for the overall system.

To investigate the operating behavior for AEM electrolyzers, tests were carried out at the green hydrogen laboratory at the Solar Research Laboratory of the Universidade Federal de Santa Catarina (Fotovoltaica/UFSC - www.fotovoltaica.ufsc.br). The goal of the investigations is to establish a level of understanding that will allow the development of an initial control algorithm for the efficient operation of the overall system. The algorithm controls a grid-independent system consisting of PV, AEM electrolyzers and buffer Li-ion batteries (both second-life and new batteries). It is particularly important to understand the extent to which startup phases and the resulting energy demand in different operating states affect overall efficiency.

2. METHODS AND MATERIALS

2.1 Green hydrogen laboratory at the Fotovoltaica/UFSC

The green hydrogen laboratory at Fotovoltaica/UFSC is designed to study battery buffered PV hydrogen production and to optimize future systems. For this purpose, the laboratory (image and schematics presented in Fig. 2 and Fig. 3) is equipped with PV modules with a total power of 500 kWp. The power is converted to alternate current and fed into the laboratory's power management system. In order to be able to carry out experiments over longer periods of time and independent of solar radiation, power can also be drawn from the grid. Two battery energy storage systems (BESS) of 100 kWh each can be used for energy buffering: 100 kWh with new Li-ion batteries and a second 100kWh BESS with second-life batteries. This allows studying the behavior of second-life batteries in such a system, especially their specific degradation behavior. The Power Management System supplies energy from the PV system, batteries, or grid to an AEM electrolyzer bank. This then produces hydrogen from this renewable energy. Rainwater is collected from the same rooftop PV systems that generate the solar electricity to run the electrolyzer, so that the building hosting the equipment is at the same time the energy and water source for water electrolysis, as shown in Fig. 2 below.

Figure 2 – The Fotovoltaica/UFSC solar energy research laboratory, with the green H2 laboratory building, which collects rainwater, produces solar electricity and houses the electrolysis system shown in the left-hand corner.
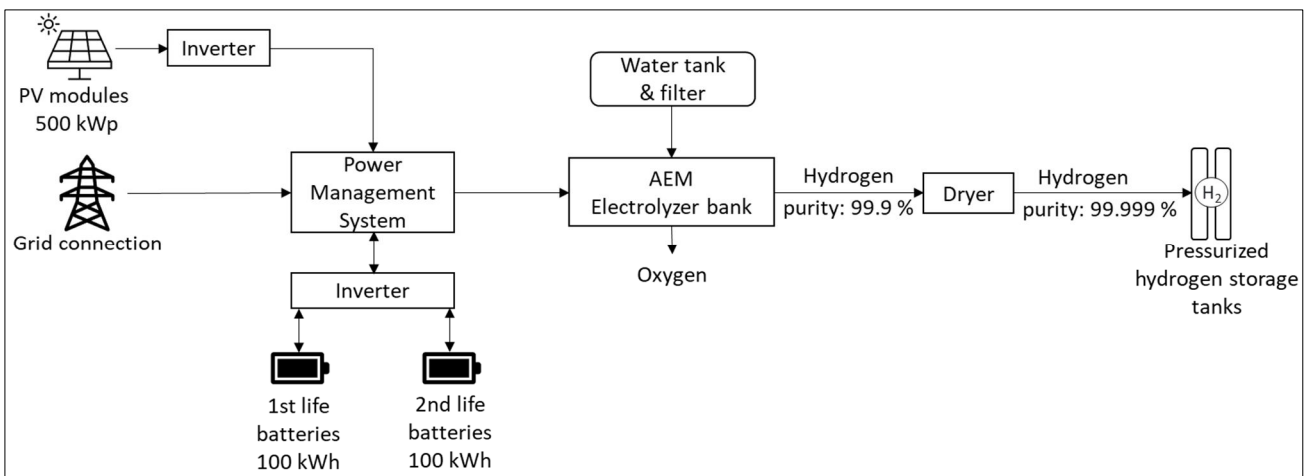

Figure 3 - Schematic view of the electrolysis system at Fotovoltaica/UFSC

AEM EL2.1 electrolyzers from Enapter® were used for the electrolysis system. According to the datasheet (Enapter (2), 2023), the operative power consumption is 2400 W, enabling a production rate of up to 500 NL_{H_2}/h. The output purity is 99,9 %. In total, nine EL2.1 electrolyzers are installed at Fotovoltaica/UFSC. To improve the purity, two Enapter DRY2.1 dryers have also been installed, as shown in Fig. 3. The dryers have an output purity of 99.999% in molar fraction and an operative power consumption of 200 W (Enapter (3), 2023). The purified hydrogen is subsequently stored in pressurized hydrogen storage tanks at up to 400 bar. There are currently two applications for the electrolysis-produced hydrogen in the laboratory: (1) direct use in fuel cells and (2) ammonia synthesis by Haber-Bosch process, with subsequent reaction with sulphuric acid to produce ammonia sulphate, which can be used as a fertilizer at the laboratory's forthcoming AgriPV project. The ammonia synthesis system was not investigated in this paper and will be described in more detail elsewhere.

Figure 4 - Electrolyzer System at the Solar Energy Laboratory Fotovoltaica/UFSC in Florianópolis, Brazil.

2.2   Analysis of the starting behavior and operative energy consumption

A single electrolyzer stack, out of the nine stacks system is examined to obtain information about the energy requirements at start up and in continuous operation. The results can later be extracted for the operation of several electrolyzers. To get a first overview, the analysis function included in the electrolyzer is used to analyze the resulting hydrogen flow and the total amount of hydrogen produced. This function allows a series of recorded operating data to be output with a minimal time increment of 1 second for a defined period of time. The values of hydrogen flow rate and total produced hydrogen are not measured directly but are calculated based on internally measured parameters. High precision is not guaranteed in this way, and mass-flow meters will be incorporated in the near future to increase precision. However, this accuracy is sufficient for the initial investigations and for understanding the overall operation behavior. The input power is analyzed using a Fluke 435-II Energy Analyzer. The EL2.1 electrolyzer allows its power to be adjusted by changing the production rate which can be varied between 100 % (500 NL/h) and 60 % (300 NL/h). To examine the possible influences of this on startup behavior and total energy demand, the analyses are also carried out in the partial load range. The measurements started in the morning after a cooling phase of at least 10 hours at ambient temperatures of 25 to 26.5 °C.

3.   EXPERIMENTS

3.1   Startup behavior

The first analysis addressed the startup behavior of electrolyzers. This is divided into several subphases (Enapter (4), 2023). The warm-up is the time period when the electrolyte is heated up to the optimal temperature of 55 °C. The ramp-up time is the time to reach the specified production rate, which is reached at about 2/3 of the total warm-up time. The build-pressure time is the time that is needed until the operating pressure is reached, what happens at about 1/6 of the total warm-up time. These investigations focus on operating temperature and production rate. For this reason, the influence of factors such as water temperature and pressure are not investigated.

Fig. 5 shows an example of a startup process of an EL2.1 AEM electrolyzer at a specified production rate of 100 % (about 500 NL/h). The nominal production rate is reached after approx. 990 sec (16.5 min), meaning the ramp-up is complete. However, the energy requirement drops significantly after around 1260 sec (21 min). At this point, the energy-intensive part of the startup is complete. For a more detailed understanding, various factors and their influence on the starting behavior energy requirement and duration must be analyzed. These are the variations of the power ratio and the difference between a cold start and a start after a short interruption with an already increased temperature.
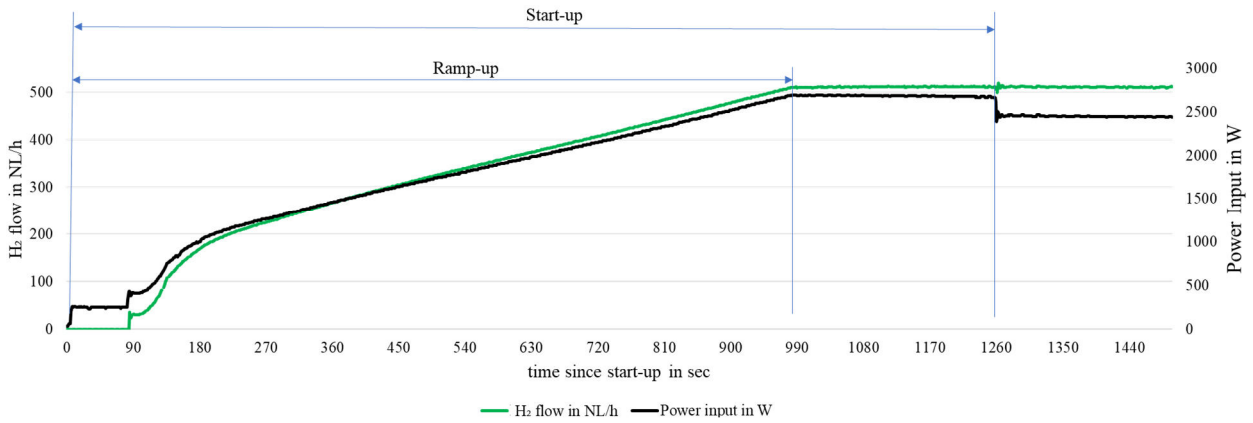
Figure 5 – Startup behavior of an AEMEL at 100 % production rate

3.2 Energy demand

To consider the power consumption of the startup of the electrolyzers in the context of a cost-efficient operation, it is necessary to investigate its influence on the total energy requirement. For this purpose, the energy required for each NL of hydrogen was calculated as a function of the operating time after startup. The lower calorific value of one NL hydrogen amounts to approximately 3 Wh (Enapter (5), 2023). Fig. 6 shows the energy consumption as a function of the start time of an electrolyzer after a cold start for a production rate of 100 %. An energy consumption of 6 Wh/NL is reached after about 470 seconds (around 8 minutes). It takes about 2530 seconds (around 42 minutes) to fall below 5 Wh/NL. In subsequent stages, the total energy requirement for hydrogen production, including the startup process, drops slightly. According to the measurement, it takes around 11,100 seconds (about 3 hours) to reach the energy consumption of 4.8 Wh/NL for a production rate of 100% as specified in the data sheet (Enapter (2), 2023).
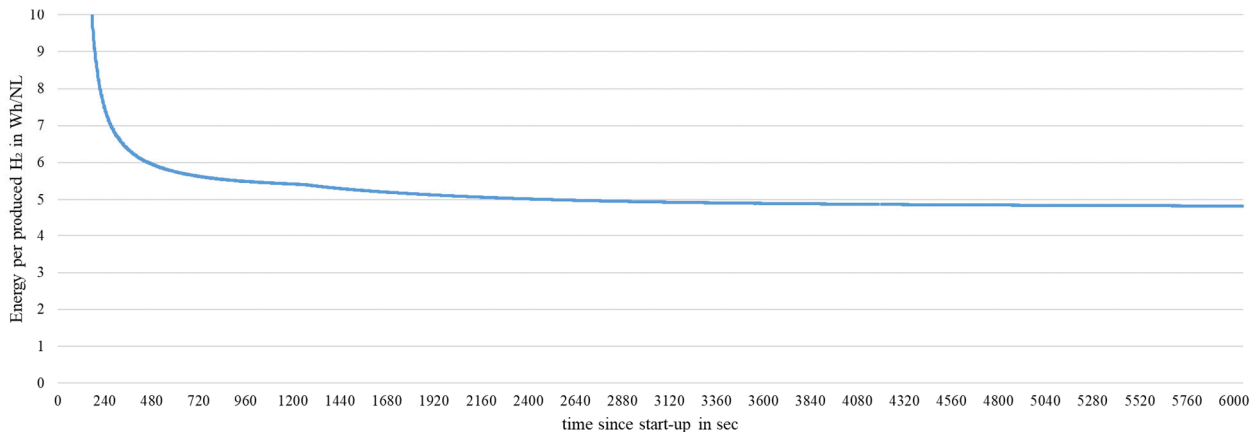

Figure 6 - Energy demand per produced hydrogen considering the starting energy of an AEMEL.

3.3 Dynamic Response

When the electrolyzer is directly coupled to an intermittent PV system, its dynamic response is of great interest. To determine how quickly the AEM electrolyzer can follow load changes, this behavior was investigated in terms of the maximum possible load changes. For this purpose, the change from a production rate of 60 % to 100 % and vice versa was examined. The tests were carried out with a sufficient time interval after start-up at working temperature. The results will be presented in chapter 4.

4. RESULTS AND DISCUSSION

The results of the power ratio variation on the operation behavior are presented in Fig. 7. In this figure, the maximum production rate of 100 %, an intermediate production rate of 80 % and the minimum production rate of 60 % were compared. It can be observed that the operation ratio has a noticeable effect on the cold start behavior in terms of power demand and ramp-up duration. The power consumption for the first 60 seconds is comparable. After that, the power consumption increases even more and there is higher power at lower production ratios than at 100 %. However, the

maximum power consumption for low production rates is significantly lower and is also reached faster. The drop in performance that marks the end of the startup phase happens at a similar point in time. The ramp-up time is directly dependent on the production rate. The higher the production rate is, the higher the ramp-up time takes. For finally reaching the nominal power (ramp-up time), the production rate of 80 % took slightly more time compared to the other investigated production rates. As shown in Fig. 7b, the hydrogen production rate also increases significantly faster at lower production ratios and reaches its maximum earlier. While only about 300 seconds (5 minutes) are required at a production rate of 60 %, reaching the total hydrogen production rate of 100 % is more than three times as long at over 960 seconds (15 minutes).
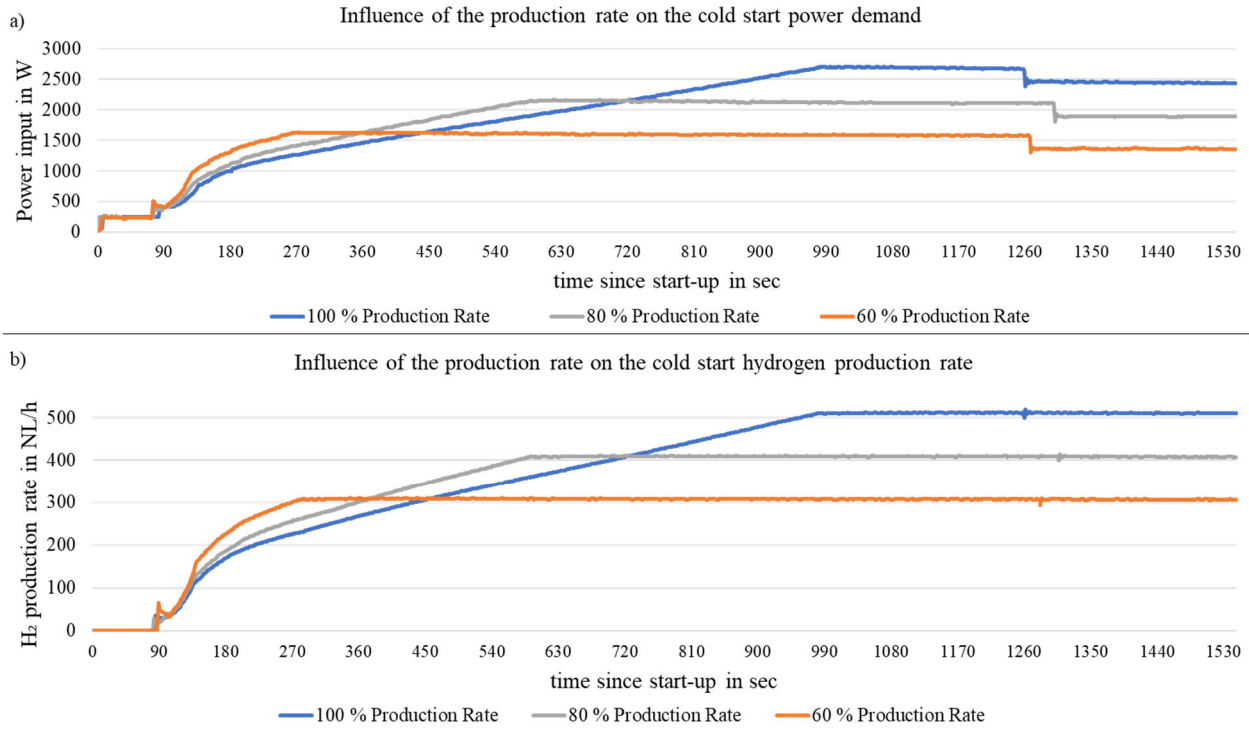
Figure 7 - Influence of the production rate on the cold start power demand (a) and cold start hydrogen flow rate (b).

The influence of the varying starting behavior due to deviating operation ratios on the total energy requirement is shown in Fig. 8. Different operation ratios do not greatly influence the energy requirement for hydrogen production in the long term. The higher the production rate, the more energy is required in the first 10 minutes. After that, the energy consumption converges. However, as the results show that higher efficiencies arise for longer operating times, the slight advantage of the lower power ratios in the first minutes is of little significance.
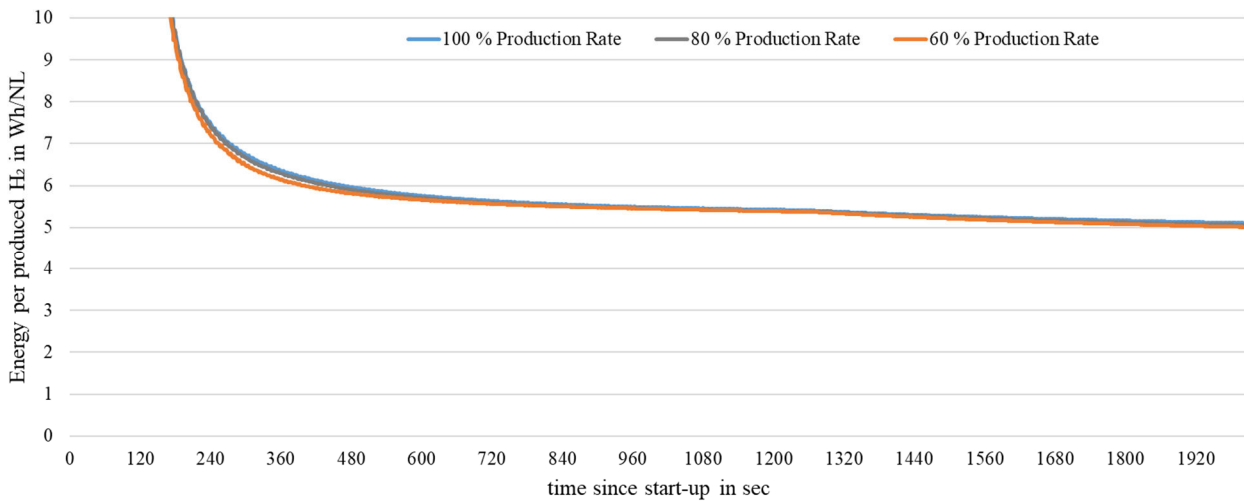

Figure 8 - Influence of the power ratio on the cold start energy demand per produced hydrogen.

To investigate the influence of the starting temperature, the electrolyzer was started at a power ratio of 100 % once in the morning at a cold start temperature of 26.5 °C and after a break of 30 and 60 minutes. After 30 minutes, the

electrolyte temperature had cooled down from 54.4 °C to 43.6 °C. After 60 minutes, it had cooled down to 38.2 °C. Fig. 9a shows the hydrogen flow rate depending on the different electrolyte temperatures. The results show that the starting temperature significantly influences the energy requirement of the ramp-up process. During a cold start, the start initially runs with lower power and a lower power increase. The start also takes significantly longer than starting with a heated electrolyte. In addition, the peak power drawn is higher after a cold start. The shorter the cooldown, the faster the maximum power is reached, and the less energy has to be expended. A similar behavior can be seen with the hydrogen flow rate (Fig. 9b). The higher the electrolyte temperature is at the start; the faster hydrogen production begins and the faster it reaches its maximum value. After a cooldown of 30 minutes, the total hydrogen production rate is reached after 300 seconds (5 minutes). After a cold start, it takes around 840 seconds (14 minutes).
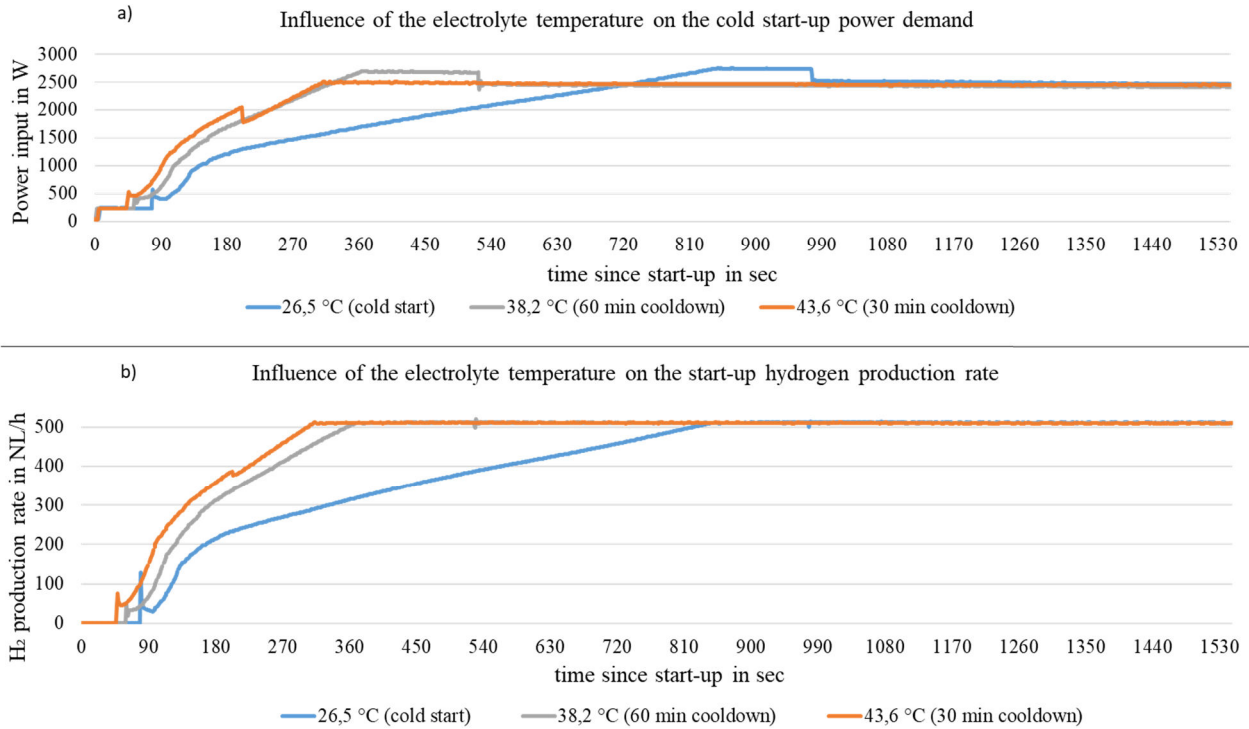

Figure 9 - Influence of the initial electrolyte temperature on the startup power demand (a) and hydrogen flow rate (b).

The measured influence of the electrolyte temperature on the starting behavior also has a noticeable effect on the energy requirements for the hydrogen produced, as shown in Fig. 10. The significantly lower energy demand for preheated electrolyte during start-up is particularly noticeable in the first few minutes of operation. The longer the idle phase was, the more energy had to be used in the first few minutes to restore hydrogen production. However, the influence of these effects is small for more extended periods.
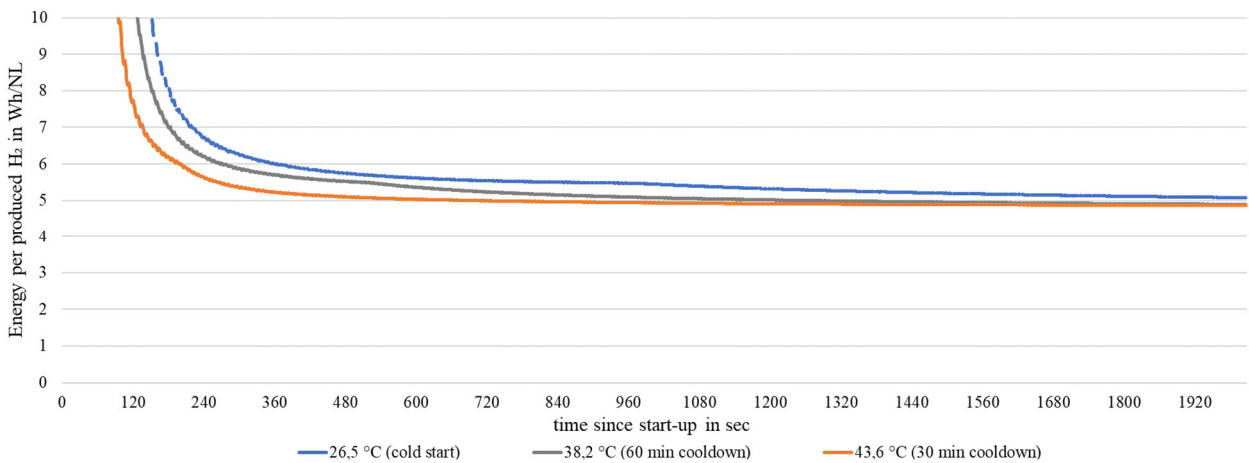

Figure 10 - Influence of the initial electrolyte temperature on the start-up energy demand per produced hydrogen.

Finally, the dynamic behavior of the AEMEL was analyzed. A reduction in the production rate from 100 % to 60 % (Fig. 11a) is proceeded nearly instantly. After less than 5 seconds the major change of hydrogen flow and power input is completed. The final hydrogen flow rate of around 311 NL/h and input power of about 1400 W is reached within

100 seconds. As shown in Fig. 11b, the increase of the production rate from 60 % to 100 % is also carried out within a short duration. However, for this increase in production rate, it takes nearly 90 seconds for the majority of the power and hydrogen flow to be reached. Full power and production rate are reached after about 180 seconds. Both increasing and decreasing the production rate do not require much energy for processes other than hydrogen production. This is an important conclusion since the time of response of different operation points determines how well the electrolyzer can respond to variations in the PV output due to clouds. The control algorithm has to take this time into account when scheduling variations in the operation of the equipment.
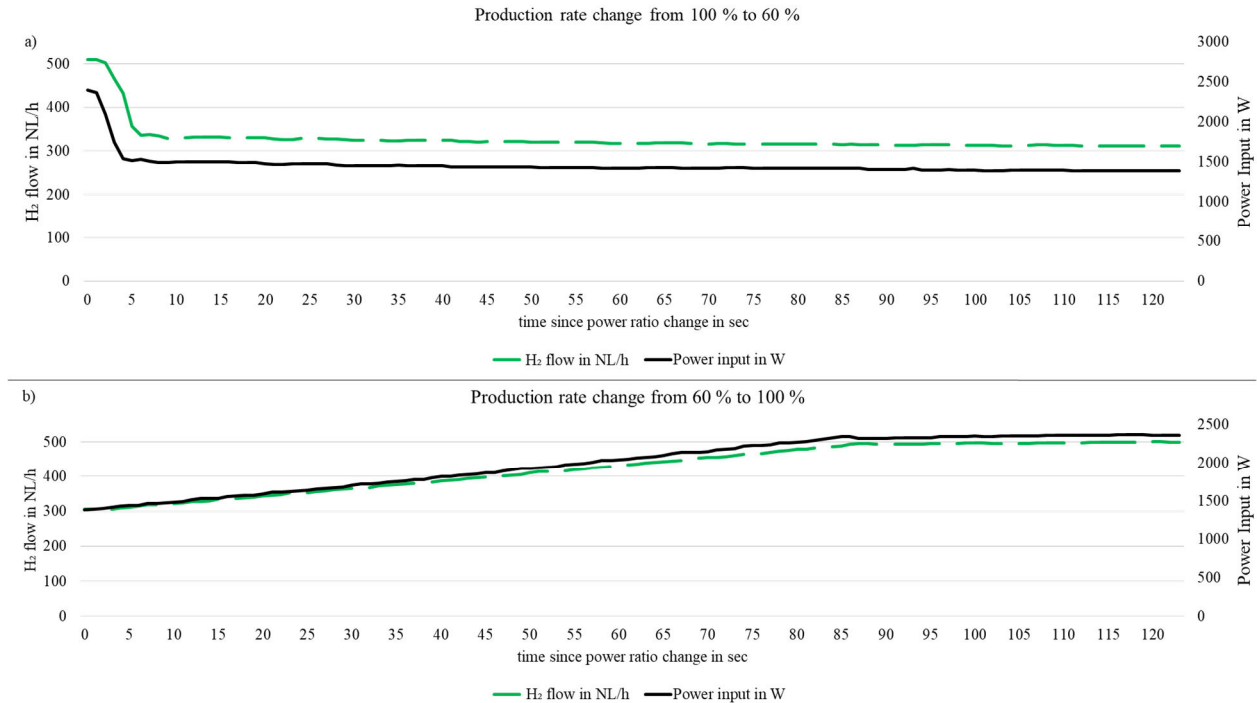

Figure 11 - Influence of the change of the production rate from 100 % to 60 % (a) and from 60 % to 100 % (b) at operating temperature on the power demand and hydrogen flow.

5. CONCLUSIONS

This paper provides a practical overview of hydrogen production using AEMEL and factors influencing the total energy required for hydrogen production. The results show that the amount of energy and time required to reach total hydrogen production depends significantly on the production rate and the initial electrolyte temperature. The lower the production rate and the higher the initial temperature, the faster the start-up and the lower the energy requirement. However, even after short idle periods, energy must be supplied before hydrogen production can be resumed. Continuous operation is therefore advantageous for high-efficiency electrolysis. A change in the production rate of the investigated AEMEL, both in the form of an increase and a decrease, is executed quickly and without significant losses. It is essential to consider the losses of the peripheral equipment for the optimal design of the control algorithms for the whole system. For a more detailed analysis, it is advisable to carry out an extended parameter variation of the influencing factors, such as production rate and electrolyte starting temperature, to find an operating optimum. It is also advisable to determine the most efficient production rate and use this as the basis for further investigations.

It should be noted that the hydrogen flow measurements were made without mass-flow meters and with the built-in analysis function of the electrolyzers. To improve the accuracy of the measurements, laboratory hydrogen mass flow meters should be used in the future. More sophisticated hydrogen flow measurement equipment is needed for more reliable measurements, in addition to the electrolyzers themselves.

REFERENCES

Arsalis, A., Papanastasiou, P., Georghiou, G.E., 2022. A comparative review of lithium-ion battery and regenerative hydrogen fuel cell technologies for integration with photovoltaic applications. Renew. Energy 191, 943–960. https://doi.org/10.1016/j.renene.2022.04.075

Becker, M., Brauns, J., Turek, T., 2021. Battery-Buffered Alkaline Water Electrolysis Powered by Photovoltaics. Chem. Ing. Tech. 93, 655–663. https://doi.org/10.1002/cite.202000151

Enapter (1), 2023. Do frequent start/stop cycles and ramping affect the electrolyser's longevity or performance? [WWW Document]. Enapter. URL https://www.enapter.com/newsroom/kb_post/do-frequent-startstop-cycles-and-ramping-affect-the-electrolysers-longevity-or-performance (accessed 11.21.23).

Enapter (2), 2023. Electrolyser EL2.1 Datasheet.

Enapter (3), 2023. Dryer DRY 2.1 Datasheet.

Enapter (4), 2023. What is the duration of starting the electrolyser unti it is fully functional? How long is the warm-up/ramp-up time? [WWW Document]. URL https://www.enapter.com/faqs (accessed 11.22.23).

Enapter (5), 2023. What is the energy content of hydrogen? [WWW Document]. URL https://www.enapter.com/newsroom/kb_post/what-is-the-energy-content-of-hydrogen (accessed 11.30.23).

Falk, J., Nedjalkov, A., Angelmahr, M., Schade, W., 2020. Applying Lithium-Ion Second Life Batteries for Off-Grid Solar Powered System—A Socio-Economic Case Study for Rural Development. Z. Für Energiewirtschaft 44, 47–60. https://doi.org/10.1007/s12398-020-00273-x

Instituto de Energia e Meio Ambiente, 2022. According to IEAM, about 1 million people don't have electricity in the Amazon. Inst. Energ. E Meio Ambiente IEMA. URL https://energiaeambiente.org.br/according-to-ieam-about-1-million-people-dont-have-electricity-in-the-amazon-20220621 (accessed 11.17.23).

Khan, M.A., Zhao, H., Zou, W., Chen, Z., Cao, W., Fang, J., Xu, J., Zhang, L., Zhang, J., 2018. Recent Progresses in Electrocatalysts for Water Electrolysis. Electrochem. Energy Rev. 1, 483–530. https://doi.org/10.1007/s41918-018-0014-z

Kikuchi, Y., Ichikawa, T., Sugiyama, M., Koyama, M., 2019. Battery-assisted low-cost hydrogen production from solar energy: Rational target setting for future technology systems. Int. J. Hydrog. Energy 44, 1451–1465. https://doi.org/10.1016/j.ijhydene.2018.11.119

Kuckshinrichs, W., Ketelaer, T., Koj, J.C., 2017. Economic Analysis of Improved Alkaline Water Electrolysis. Front. Energy Res. 5. https://doi.org/10.3389/fenrg.2017.00001

Leduchowicz-Municio, A., López-Gozález, A., Domenech, B., Ferrer-Martí, L., Udaeta, M.E.M., Gimenes, A.L.V., 2022. Last-mile rural electrification: Lessons learned from universalization programs in Brazil and Venezuela. Energy Policy 167, 113080. https://doi.org/10.1016/j.enpol.2022.113080

Mayyas, A., Wei, M., Levis, G., 2020. Hydrogen as a long-term, large-scale energy storage solution when coupled with renewable energy sources or grids with dynamic electricity pricing schemes. Int. J. Hydrog. Energy 45, 16311–16325. https://doi.org/10.1016/j.ijhydene.2020.04.163

McKinsey, 2021. Green Hydrogen: an opportunity to create sustainable wealth in Brazil and the world [WWW Document]. URL https://www.mckinsey.com/br/en/our-insights/hidrogenio-verde-uma-oportunidade-de-geracao-de-riqueza-com-sustentabilidade-para-o-brasil-e-o-mundo#/ (accessed 11.20.23).

Neugebauer, R. (Ed.), 2022. Wasserstofftechnologien. Springer Vieweg, Wiesbaden [Heidelberg].

Oliveira, A.K.V.D., Azevedo, K.L.R.D., Santos, D.O.D., Aghaei, M., Rüther, R., Orabona, R., Naspolini, H., 2023. Assessing the Potential of Green Hydrogen in Decarbonizing Off-Grid Amazonian Communities, in: 2023 International Conference on Future Energy Solutions (FES). Presented at the 2023 International Conference on Future Energy Solutions (FES), IEEE, Vaasa, Finland, pp. 1–6. https://doi.org/10.1109/FES57669.2023.10182925

Papadopoulos, V., Desmet, J., Knockaert, J., Develder, C., 2018. Improving the utilization factor of a PEM electrolyzer powered by a 15 MW PV park by combining wind power and battery storage – Feasibility study. Int. J. Hydrog. Energy 43, 16468–16478. https://doi.org/10.1016/j.ijhydene.2018.07.069

Shiva Kumar, S., Himabindu, V., 2019. Hydrogen production by PEM water electrolysis – A review. Mater. Sci. Energy Technol. 2, 442–454. https://doi.org/10.1016/j.mset.2019.03.002

Shiva Kumar, S., Lim, H., 2022. An overview of water electrolysis technologies for green hydrogen production. Energy Rep. 8, 13793–13813. https://doi.org/10.1016/j.egyr.2022.10.127

Silva, S.B., Severino, M.M., De Oliveira, M.A.G., 2013. A stand-alone hybrid photovoltaic, fuel cell and battery system: A case study of Tocantins, Brazil. Renew. Energy 57, 384–389. https://doi.org/10.1016/j.renene.2013.02.004

Tebibel, H., Khellaf, A., Menia, S., Nouicer, I., 2017. Design, modelling and optimal power and hydrogen management strategy of an off grid PV system for hydrogen production using methanol electrolysis. Int. J. Hydrog. Energy 42, 14950–14967. https://doi.org/10.1016/j.ijhydene.2017.05.010

Zeyen, E., Victoria, M., Brown, T., 2023. Endogenous learning for green hydrogen in a sector-coupled energy model for Europe. Nat. Commun. 14, 3743. https://doi.org/10.1038/s41467-023-39397-2

Zhao, Y., Pohl, O., Bhatt, A.I., Collis, G.E., Mahon, P.J., Rüther, T., Hollenkamp, A.F., 2021. A Review on Battery Market Trends, Second-Life Reuse, and Recycling. Sustain. Chem. 2, 167–205. https://doi.org/10.3390/suschem2010011